Collapse of Landau levels in Weyl semimetals

Vicente Arjona[1], Eduardo V. Castro[2,3], and María A. H. Vozmediano [1]

[1] *Instituto de Ciencia de Materiales de Madrid, and CSIC, Cantoblanco, 28049 Madrid, Spain*
[2] *CeFEMA, Instituto Superior Técnico, Universidade de Lisboa,*
Av. Rovisco Pais, 1049-001 Lisboa, Portugal and
[3] *Beijing Computational Science Research Center, Beijing 100084, China*

It is known that in two dimensional relativistic Dirac systems, the Landau levels can collapse in the presence of a critical in-plane electric field. We extend this mechanism to the three dimensional Weyl semimetals and analyze the physical consequences for the cases of both, real and pseudo Landau levels arising form strain–induced elastic magnetic fields.

I. INTRODUCTION

Graphene and Weyl semimetals (WSM) are examples of Dirac matter in two and three dimensions respectively. In both materials, the Fermi surface consists on a series of pairs of points of definite chirality, located at different positions in the Brillouin zone. The relativistic nature of these systems has important experimental consequences. One of the best explored in the literature is the behavior in magnetic fields. The Landau level (LL) spectrum differs from that of the standard electron systems and the LL structure was the compelling evidence of having Dirac electrons in graphene [1, 2]. The characteristic zeroth Landau level LL plays an important role in the discussion of the chiral anomaly in WSM [3] in the 3D systems and the magneto-resistance has become the standard test of the anomaly [4–9].

More recently it has been recognized that, as happens in graphene, elastic lattice deformations couple to the low energy electronic excitations of WSM in the form of elastic axial gauge fields [10]. The original derivation was followed by a number of works extracting the consequences of this new vector coupling [11–15]. Strain engineering can give rise to pseudo LL in these 3D materials, nice examples are provided in refs. [11, 13] and a general analysis of strain induced LL in any dimension has been presented in [16].

In this work we analyze the spectrum of WSM in the presence of perpendicular electric and magnetic fields. The motivation lies on the recognition that, for Dirac materials, the presence of a critical electric field perpendicular to the magnetic field induces a collapse of the Landau levels. This fact was explicitly derived in two spacial dimensions for the case of graphene in [17, 18], and has also been recognized in a different context in [19, 20] when analyzing tilted WSM. Our main contribution concerns the strained WSM. The critical observation is that, in addition to the elastic gauge fields, strain gives rise in general to a deformation potential that acts as a pseudo–electric field perpendicular to the pseudo–magnetic field leading to the collapse of the pseudo Landau levels (PLL). This phenomena has been discussed for graphene in [21]. To fix the notation we will first derive the condition for the
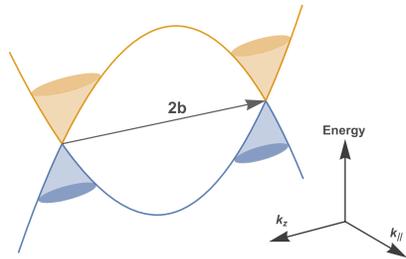
FIG. 1: Schematic representation of the band structure of eq. (1) with the Weyl nodes separation chosen along the k_z axis. $k_\parallel$ stands for (k_x, k_y).

collapse of LL in the case of real electromagnetic fields in Sec. II and then examine the situation of the electronic oscillations induced by elastic deformation in Sec. III. We end in Sec. IV with some further considerations on the effects of strain in WSM.

II. COLLAPSE OF THE LANDAU LEVELS IN WEYL SEMIMETALS. ELECTROMAGNETIC FIELDS

Dirac fermions in three dimensions are described by a four component spinor wave function obeying the Dirac equation $(\gamma^\mu \partial_\mu - m)\Psi = 0$. In the massless case and choosing the Weyl representation for the Dirac matrices, the equation splits into two equations with two-component wave functions representing Weyl fermions of oposite chirality. In the material realization of the Weyl physics, the two chiralities (band crossings) are separated in k space by a vector $b^\mu (\mu = 0, 1, 2, 3)$. The minimal low energy effective model describing a WSM with only two nodes, is

$$\mathcal{L} = \bar{\Psi}\gamma^\mu(\partial_\mu + i\gamma^5 b_\mu)\Psi, \tag{1}$$

where γ^μ are standard Dirac matrices. The vector b_μ breaks Lorentz symmetry. Its time component b_0 is related to the separation in energy of the Weyl nodes and breaks, in addition, inversion symmetry. The spacial component b_i represents the separation in k space

and breaks time reversal symmetry $\mathcal{T}$. Fig. 1 shows a schematic representation of the band structure of eq. (1) with the vector $\vec{b}$ pointing in the z direction.

Inversion-broken WSM have been found experimentally [9, 22, 23]; $\mathcal{T}$ broken have been predicted in magnetic compounds [24] and experimental evidences are advocated in [25].

Signatures of the chiral anomaly are found in the behavior of the magnetorresistance in parallel E and B fields. The case of perpendicular E and B fields has been less studied although a very interesting discussion of the LL spectrum in the context of tilted Weyl semimetals is done in refs. [19, 20]. The LL collapse is already implicit there but their aim is different. We will present here the derivation of the LL collapse in perpendicular electric and magnetic field to fix the notation and to pave the way for the discussion of strain in the next section.

Around a single Weyl node, the WSM is a relativistic system with the velocity of light c replaced by the Fermi velocity v_F. As we know from special relativity [26, 27], a boost in the direction perpendicular to E and B with the appropriate velocity leads to a reference frame where the electric field E' vanishes. The spectrum of a WSM in perpendicular E and B is obtained by solving the problem in the primed reference frame with magnetic field B' and boosting back to the original reference frame. This was done in the 2D case in ref. [17]. The 3D derivation is as follows:

We choose the Landau gauge $\mathbf{A} = (-By, 0, 0)$ and the scalar potential $\phi = -Ey$. This represents a constant magnetic and electric fields $\mathbf{B}, \mathbf{E}$ pointing in the z and y directions respectively. Since k_z is a good quantum number, the system can be considered as a collection of 2D Dirac layers in a perpendicular electromagnetic field. The energy spectrum of such configuration is well known; electron motion is arranged into Landau levels:

$$\epsilon_n = \pm\sqrt{\Omega_c^2 n + v_f^2 k_z^2}, \qquad (2)$$

where the cyclotron frequency in units $\hbar = 1$ is $\Omega_c = \sqrt{2}v_F/l_B$, with $l_B = \sqrt{1/(eB)}$ the magnetic length. Under a boost in the x direction with velocity v, the chosen electromagnetic field transforms as:

$$E'_y = \gamma(E_y - vB_z) \quad , \quad B'_z = \gamma(B_z - \frac{v}{v_F^2}E_y), \qquad (3)$$

where $\gamma = 1/\sqrt{1-\beta^2}$, $\beta = v/v_F$. When the velocity coincides with the drift velocity, $v_d = E/B$, the primed reference frame experiences only a magnetic field of magnitude $B'_z = \sqrt{1-\beta^2}B$ and the spectrum is given by eq. (2) with the primed magnetic field and with $\beta = E/v_F B$. Since the energy is the zeroth component of the energy-momentum quadrivector, the inverse boost transformation

$$\epsilon_n = \gamma(1-\beta^2)\epsilon'_n + v_f \beta k_x \qquad (4)$$
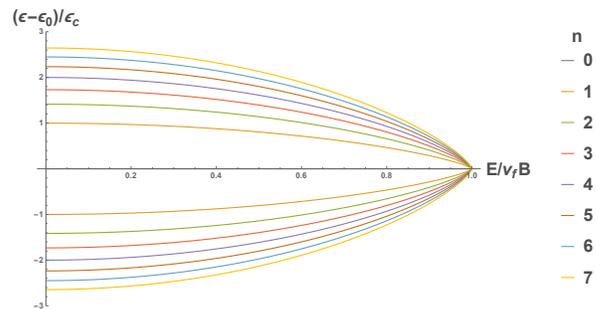
FIG. 2: Cyclotron frequency as a function of the electric field for $k_z=0$.

gives the spectrum in the original frame. The final expression is

$$\epsilon_n = \pm\sqrt{\Omega_c^2 n(1-\beta^2)^{3/2} + v_f^2 k_z^2(1-\beta^2)} + v_f \beta k_x. \quad (5)$$

For comparison, the spectrum of a non-relativistic electron system in the same field configuration is

$$\epsilon_n = \left(n + \frac{1}{2}\right)\omega_c + \frac{k_z^2}{2m} - k_y\frac{E}{B} - \frac{m}{2}\left(\frac{E}{B}\right)^2, \qquad (6)$$

with the cyclotron frequency given by the standard expression $\omega_c = eB/mc$. As it happens in the 2D case [17, 18], apart from a rigid shift of the levels (which is the only effect of the electric field in the case of the non-relativistic electron system), there is a non trivial dependence of the cyclotron frequency with the electric field. The evolution of the cyclotron frequency with the applied electric field for $k_z = 0$ is shown in Fig. 2. As it can be seen, the LL collapse for the critical value $E = v_F B$. The LL collapse described here is different from the overlap of LL occurring in a non relativistic electron gas [28]. It is a property of the Dirac matter that will take place not only in WSM but also in Dirac semimetals. These materials have the two chiral nodes located at the same point in the Brillouin zone and are, at present, more accesible experimentally. Examples are Na_3Bi or Cd_3As_2 [8, 29, 30]. Three dimensional Dirac LL have already been observed in these compounds so it would be interesting to check the LL collapse in these materials. Although indications of LL collapse have been obtained experimentally [31, 32] we do not know of similar attempts in 3D samples.

III. STRAIN IN WEYL SEMIMETALS: COLLAPSE OF THE PSEUDO LANDAU LEVELS

The coupling of electronic excitations to lattice deformations in graphene in the form of gauge fields [33–35], the prediction of pseudo Landau levels (PLL) for some strain configurations [36, 37], and their experimental observation with Scanning Tuneling Spectroscopy [38] have
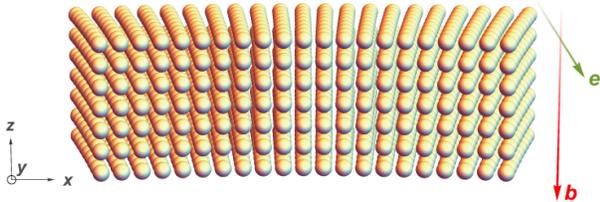
FIG. 3: Sketch of a sheet of the proposed rectangular lattice WSM. The applied strain configuration bends the original system into a circular arc in the x-y plane. This configuration is able to produce both pseudo–magnetic and pseudo–electric fields, the PLL spectrum collapsing when the critical value is reached.

been one of the most exotic and fruitful developments in the physics of graphene. The concept of elastic gauge fields and the capability to manipulate the electronic excitations by means of strain (straintronics) has been later extended to other more general 2D Dirac materials [39]. Massless Dirac nodes must come in pairs of opposite chirality [40]. The general understanding is that elastic gauge fields will arise when these Dirac nodes are located at non equivalent points in the Brillouin zone [41]. Weyl semimetals share most of the relevant properties of graphene concerning the coupling of elastic and electronic degrees of freedom. The fact that elastic gauge fields would also be present in WSM was deduced in a recent publication [10]. In this section we will explore the collapse of the PLL in certain strain configurations due to the strain induced deformation potential following the lines described for graphene in [21].

Elastic lattice deformations are parametrized by the strain tensor $u_{ij} = 1/2(\partial_i u_j + \partial_j u_i)$, a function of the displacement vector u_i. A symmetry approach allows a straightforward construction of an elastic gauge field as $A_i^{el} = u_{ij}b_j$ $(i,j = x,y,z)$. The coupling parameters must be fixed either by a microscopic model (tight binding, *ab initio*) or determined by experiments. In the original reference [10], these were extracted from a tight-binding model.

Another important electron-phonon coupling in elasticity theory is the deformation potential (shifts in the energy bands resulting from deformations of the crystal lattice). It is proportional to the trace of the strain tensor and is of the same order as the elastic gauge field in a derivative expansion. Considering the simplest case of two Weyl nodes separated in momentum space, the low energy Hamiltonian around one of the Weyl nodes coupled to the lattice deformation is

$$\mathcal{H} = v_F \sigma^i (p_i + cA_i) + g\Phi\mathbb{1}, \qquad (7)$$

where $\Phi(x) \sim \sum_j u_{jj}(x)$ and g is the coupling constant associated to the deformation potential. The dimensionless Grüneisen parameter c is typically of order one in most materials [42, 43]. In what follows we will put $c = 1$ and remove it from the discussion. The deformation potential couples as a scalar electromagnetic potential which can give rise to a (pseudo) electric field $E_i = -\partial_i \Phi$. Next we will demonstrate the collapse of the PLL in a very simple configuration and later we will discuss more realistic examples.

Assume that we have a WSM with two Weyl nodes separated a distance b in the k_x direction. A strain configuration such that $u_{xx} = -By/b, u_{yy} = u_{zz} = 0$, will give rise to an elastic vector potential $A_i = u_{ij}b_j$ such that $A_x = -By$, $A_y = A_z = 0$. This describes a uniform magnetic field of magnitude B in the z direction. Simultaneously, the scalar potential $\Phi = -gyB/b$, induces a pseudo–electric field of magnitude $E = gB/b$ pointing in the y direction. We are then in the situation described in the previous section. The collapse of the PLL occurs when $E \geq v_F B$, i. e. $gB/b \geq v_F B$. The condition for the PLL collapse translates into a constraint on the values of the coupling constant associated to the deformation potential: $g \geq v_F b$. Although there are not yet measurements of the electron–phonon couplings in WSM, using reasonable numbers we see that the condition will be easily attainable in the samples. The separation between the nodes is estimated to be $b \sim 0.08 \text{Å}^{-1}$ in $TaAs$, with the Fermi velocity $v_F \sim 1.3 \times 10^5 m/s$ [44]. These values give a lower bound for the elastic coupling constant of $g \geq 0.07 eV$ meaning that the samples will typically be affected by the effect described. Notice that the estimated value in graphene is of the order of 4 eV taking screening into account. Thin films of WSM which are the ones more suitable for straintronics are not expected to be so deformable but the required value is fifty times smaller and screening is reduced in WSM due to the relativistic spectrum.

Apart from the academic example presented to expose the phenomenon, more realistic strain configurations will also be affected by it and this effect will have to be taken into account for a correct interpretation of the experiments when these are available. Since the deformation potential is the trace of the strain tensor, shear strain conserving the volume of the sample will not generate a pseudo–electric field. This is the case for example of the torsional strain discussed in [11] or the tetra-axial strain in the diamond lattice of ref. [16]. Other strain configurations easier to implement experimentally will be fully affected by the effect. The best experimentally accessible devices will be obtained by bending thin films of WSM, a generalization of the strain configuration first suggested in ref. [37] for graphene sheets. Consider a rectangular lattice model with the Weyl nodes separated by a distance b in the k_x direction. A generic deformation

$$\begin{aligned} u_x &= u_0(2xy + Cx) \\ u_y &= u_0[-x^2 - Dy(y + C)] \\ u_z &= 0, \end{aligned} \qquad (8)$$

where u_0 and D are constants that depend on the material; u_0 defines the maximum stress and D is a relation between Lamé coefficients. C parametrizes a family of deformations encoding the same pseudomagnetic field. The strain configuration (8) gives rise to the elastic gauge potential $A_x = u_{xx}b_x = u_0(2y+C)b$. The constant pseudo–magnetic field will be $B_z = -2u_0 b$. In addition to the pseudo–magnetic field, this strain configuration has a deformation potential $\Phi(y) = u_0(1-D)(2y+C)$ that will generate a constant pseudo–electric field $E_y = -2u_0(1-D)g$ perpendicular to the magnetic field, as shown in Fig. 3. As in the above example, the collapse of the PLL spectrum is translated into a restriction for the values of the elastic coupling constants, $g \geq v_f b/(1-D)$. For a thin film of Cd_3As_2 as the one suggested in ref. [13], a coupling constant $g \geq 0.16eV$, would be needed to collapse the predicted oscillations.

IV. DISCUSSION

This work can be extended to situations involving more general – and more realistic – materials. In particular, most of the actual WSM are inversion broken, meaning that the inequivalent Weyl nodes are separated in energy by a zeroth component of the b field in eq. (1). In a recent publication [45] it was shown that, in these materials, a time component of the elastic gauge field will develop under strain. This gives rise to a pseudo–electric gauge field that, in contrast to the one associated to the deformation potential, will be axial, i. e. will couple with opposite sign to the two Weyl nodes of opposite chirality. The addition of the two terms can lead to interesting situations where the chiral imbalance is maximized by making the total scalar potential zero in one of the nodes.

The Dirac semimetals have been the subject of intense experimental research and the measures of the magneto-resistance have been used as an experimental evidence of the chiral magnetic effect [46, 47]. Even though these materials will not support elastic gauge fields, strain will still induce a deformation potential that will also affect the spectrum of the system in real magnetic fields.

[1] Novoselov, K. S. *et al.* Two-dimensional gas of massless dirac fermions in graphene. *Nature* **438**, 197 (2005).

[2] Zhang, Y., Tan, Y.-W., Stormer, H. L. & Kim, P. Experimental observation of the quantum hall effect and berry's phase in graphene. *Nature* **438**, 201 (2005).

[3] Nielsen, H. B. & Ninomiya, M. The Adler-Bell-Jackiw anomaly and Weyl fermions in a crystal. *Phys. Lett. B* **130**, 389 (1983).

[4] Burkov, A. A. Chiral anomaly and transport in Weyl metals. *Journal of Physics: Condensed Matter* **27**, 113201 (2015).

[5] Jia, S., Xu, S. & Hasan, M. Z. Weyl semimetals, fermi arcs and chiral anomalies. *Nature Materials* **15**, 1140 (2016).

[6] Li, C. *et al.* Giant negative magnetoresistance induced by the chiral anomaly in individual Cd3As2 nanowires. *Nat. Comm.* **6**, 10137 (2015).

[7] Huang, X. *et al.* Observation of the chiral-anomaly-induced negative magnetoresistance in 3d weyl semimetal taas. *Phys. Rev. X* **5**, 031023 (2015).

[8] Xiong, J. *et al.* Evidence for the chiral anomaly in the dirac semimetal Na_3Bi. *Science* **350**, 413 (2015).

[9] Zhang, C. *et al.* Signatures of the Adler Bell Jackiw chiral anomaly in a Weyl fermion semimetal. *Nat. Comm.* **7**, 10735 (2016).

[10] Cortijo, A., Ferreiros, Y., Landsteiner, K. & Vozmediano, M. A. H. Elastic gauge fields in Weyl semimetals. *Phys. Rev. Lett.* **115**, 177202 (2015).

[11] Pikulin, D. I., Chen, A. & Franz, M. Chiral anomaly from strain-induced gauge fields in dirac and weyl semimetals. *Phys. Rev. X* **6**, 041021 (2016).

[12] Grushin, A. G., Venderbos, J. W. F., Vishwanath, A. & Ilan, R. Inhomogeneous weyl and dirac semimetals: Transport in axial magnetic fields and fermi arc surface states from pseudo-landau levels. *Phys. Rev. X* **6**, 041046 (2016).

[13] Liu, T., Pikulin, D. I. & Franz, M. Quantum oscillations without magnetic field. *Phys. Rev. B* **95**, 041201 (2017).

[14] Varjas, D., Grushin, A. G., Ilan, R. & Moore, J. E. Dynamical piezoelectric and magnetopiezoelectric effects in polar metals from berry phases and orbital moments. *Phys. Rev. Lett.* **117**, 257601 (2016).

[15] Guan, S. *et al.* Strain effects on dirac semimetals: Artificial fields and topological phase transitions. *arXiv1609.00615* (2016).

[16] Rachel, S., Göthel, I., Arovas, D. P. & Vojta, M. Strain-induced landau levels in arbitrary dimensions with an exact spectrum. *Phys. Rev. Lett.* **117**, 266801 (2016).

[17] Lukose, V., Shankar, R. & Baskaran, G. Novel electric field effects on landau levels in graphene. *Phys. Rev. Lett.* **98**, 116802 (2007).

[18] Peres, N. M. R. & Castro, E. V. Algebraic solution of a graphene layer in transverse electric and perpendicular magnetic fields. *Journal of Physics: Condensed Matter* **19**, 406231 (2007).

[19] Yu, Z.-M., Yao, Y. & Yang, S. A. Predicted unusual magnetoresponse in Type-II weyl semimetals. *Phys. Rev. Lett.* **117**, 077202 (2016).

[20] Tchoumakov, S., Civelli, M. & Goerbig, M. O. Magnetic-field-induced relativistic properties in Type-I and Type-II Weyl semimetals. *Phys. Rev. Lett.* **117**, 086402 (2016).

[21] Castro, E. V., Cazalilla, M. A. & Vozmediano, M. A. H. Raise and collapse of strain-induced pseudo-Landau levels in graphene. *ArXiv e-prints* (2016). 1610.08988.

[22] Lv, B. Q. *et al.* Experimental discovery of Weyl semimetal $TaAs$. *Phys. Rev. X* **5**, 031013 (2015).

[23] Xu, S. Y. *et al.* Observation of fermi arc surface states in a topological metal: A new type of 2d electron gas beyond Z_2 topological insulators. *Science* **347**, 294 (2015).

[24] Chang, G. *et al.* A strongly robust type ii weyl fermion semimetal state in Ta_3S_2. *Science Advances* **2** (2016).

[25] Borisenko, S. *et al.* Time-reversal symmetry breaking weyl state in Yb Mn Bi_2. *arXiv:1507.04847* (2015).

[26] Landau, L. & Lifshitz, E. *The Classical Theory of Fields* (Pergamon Press, 1971). Volume 2 of A Course of Theoretical Physics.

[27] Jackson, J. D. *Classical Electrodynamics* (Wiley, 1998).

[28] Kramer, T., Bracher, C. & Kleber, M. Electron propagation in crossed magnetic and electric fields. *Journal of Optics B: Quantum and Semiclassical Optics* **6**, 21 (2004).

[29] Liu, Z. K. *et al.* Discovery of a three-dimensional topological dirac semimetal Na_3Bi. *Science* **343**, 864 (2014).

[30] Jeon, S. *et al.* Landau quantization and quasiparticle interference in the three dimensional dirac semimetal ?Cd_3As_2. *Nature Materials* **13**, 851 (2014).

[31] Singh, V. & Deshmukh, M. M. Nonequilibrium breakdown of quantum hall state in graphene. *Phys. Rev. B* **80**, 081404 (2009).

[32] Gu, N., Rudner, M., Young, A., Kim, P. & Levitov, L. Collapse of landau levels in gated graphene structures. *Phys. Rev. Lett.* **106**, 066601 (2011).

[33] Kane, C. L. & Mele, E. J. Size, shape, and low energy electronic structure of carbon nanotubes. *Phys. Rev. Lett.* **78**, 1932–1935 (1997).

[34] Suzuura, H. & Ando, T. Phonons and electron-phonon scattering in carbon nanotubes. *Phys. Rev. B* **65**, 235412 (2002).

[35] Vozmediano, M. A. H., Katsnelson, M. I. & Guinea, F. Gauge fields in graphene. *Physics Repports* **493**, 109 (2010).

[36] Guinea, F., Katsnelson, M. I. & Geim, A. G. Energy gaps, topological insulator state and zero-field quantum hall effect in graphene by engineering. *Nature Physics* **6**, 30 (2010).

[37] Guinea, F., Geim, A. K., Katsnelson, M. I. & Novoselov, K. S. Generating quantizing pseudomagnetic fields by bending graphene ribbons. *Phys. Rev. B* **81**, 035408 (2010).

[38] Levy, N. *et al.* Strain induced pseudo magnetic fields greater than 300 tesla in graphene nanobubbles. *Science* **329**, 544 (2010).

[39] Amorim, B. *et al.* Novel effects of strains in graphene and other two dimensional materials. *Physics Reports* **617**, 1 (2016).

[40] Nielsen, H. B. & Ninomiya, M. Absence of neutrinos on a lattice: (i). proof by homotopy theory. *Nuc. Phys. B* **185**, 20–40 (1981).

[41] Cortijo, A., Ferreiros, Y., Landsteiner, K. & Vozmediano, M. A. H. Visco elasticity in 2d materials. *2D Materials* **3**, 011002 (2016).

[42] Hofmeister, A. M. & Mao, H. Redefinition of the mode gruneisen parameter for polyatomic substances and thermodynamic implications. *PNAS* **99**, 559 (2002).

[43] Ibach, H. & *Lth*, H. *Solid-State Physics: An Introduction to Principles of Materials Science* (Springer Science and Business Media, 2009).

[44] Hasan, M. Z., Xu, S. Y., Belopolski, I. & Huang, S. Discovery of weyl fermion semimetals and topological fermi arc states. *Ann. Rev. of Cond. Mat. Phys.* (2017).

[45] Cortijo, A., Kharzeev, Y., Landsteiner, K. & Vozmediano, M. A. H. Strain induced chiral magnetic effect in Weyl semimetals. *Phys. Rev. B* **95**, 241405(R) (2016).

[46] Fukushima, K., Kharzeev, D. E. & Warringa, H. J. Chiral magnetic effect. *Phys. Rev. D* **85**, 045104 (2008).

[47] Li, Q., Kharzeev, D. *et al.* Chiral magnetic effect in $ZrTe_5$. *Nat. Phys.* **10**, 3648 (2016).